

A semi-analytic seasonal algorithm to retrieve chlorophyll-*a* concentration in the Northwest Atlantic Ocean from SeaWiFS data

E. Devred^{1,2,*}, C. Fuentes-Yaco^{1,2}, S. Sathyendranath^{1,2}, C. Caverhill², H. Maass², V. Stuart^{1,2},
T. Platt² & G. White²

¹Department of Oceanography, Dalhousie University, Halifax, Nova Scotia, Canada B3H 4J1, Canada.

²Biological Oceanography Division, Bedford Institute of Oceanography, Box 1006, Dartmouth, Nova Scotia, B2Y 4A2, Canada

*[E-mail: DevredE@mar.dfo-mpo.gc.ca]

Received 1 November 2004, revised 27 June 2005

In a companion paper [Fuentes-Yaco *et al.*, *Indian J. Mar. Sci.*, 34(2005), 341-355], it was demonstrated that the SeaWiFS OC4 algorithm, applied to the Northwest Atlantic, resulted in a systematic bias in the retrieved chlorophyll-*a* concentration. Their comparison of satellite-derived chlorophyll-*a* values with matching *in situ* observations showed that the OC4 algorithm as implemented in the NASA SeaDAS software package, overestimated chlorophyll-*a* in waters with low pigment concentrations, and underestimated chlorophyll-*a* for high pigment concentrations. In this paper, we seek an explanation for the observed bias, using a semi-analytic model of ocean colour [Sathyendranath *et al.*, *Int. J. Remote Sens.*, 22(2001), 249-273] modified to account for seasonal and regional variations in the spectral absorption properties of phytoplankton, dissolved matter (yellow substances) and detritus. The model is also extended into the near infrared region to evaluate the possible impact on the atmospheric correction algorithm. The results indicate that much of the bias can be explained by local variations in the inherent optical properties of particulate and dissolved matter present in the region. The algorithm based on the semi-analytical model eliminates practically all the bias (inaccuracy) in the retrieved chlorophyll-*a* concentrations, but does not improve the precision of retrieval.

[**Key words:** Ocean colour, SeaWiFS, remote-sensing, reflectance, chlorophyll *a*, Northwest Atlantic Ocean, algorithm]

[**IPC Code:** Int.Cl.⁷ G01D 21/00, G06K 7/10]

1. Introduction

The mapping of phytoplankton concentrations in the oceans at large scales requires the use of satellites. The ocean can be observed on a daily basis with a high spatial resolution using ocean-colour sensors mounted on satellites. Applications of ocean-colour data are numerous, and include primary production, fisheries and coastal management. The interpretation and application of ocean-colour data have improved greatly in the last 25 years, since the launch of the Coastal Zone Colour Scanner (CZCS). Currently, the Sea-viewing Wide Field-of-View Sensor (SeaWiFS) data provided by the National Aeronautic and Space Administration (NASA, USA) find wide usage in the oceanographic community. NASA also provides a software package, the SeaWiFS Data Analysis System (SeaDAS) to process the raw data to retrieve geophysical variables such as chlorophyll-*a* concentration and spectral radiances and to display the results as images.

The accuracy of the retrieval of the chlorophyll-*a* concentration from space depends mainly on the ability of the algorithm i) to correct the Top of Atmosphere (TOA) signal collected by the satellite sensor for the effect of atmospheric components (gases and aerosols) for retrieval of the water-leaving radiances and ii) to relate the water-leaving radiances to the chlorophyll-*a* concentration. The goal of NASA is to reach an accuracy of $\pm 35\%$ for chlorophyll-*a* concentrations in the range between 0.05 and 30 mg m⁻³. Recent validation attempts¹ indicate that this goal is reached for chlorophyll-*a* concentrations between 0.3 and 3 mg m⁻³, but that a clear overestimation occurs at chlorophyll-*a* concentrations less than 0.3 mg m⁻³. The atmospheric correction procedure for SeaWiFS data^{2,3} uses the reflectance ratio in the near infrared to assess the contribution of aerosol particles, which is then extrapolated to the visible domain. The NASA chlorophyll-*a* algorithms are based on a large dataset (SeaWiFS Bio-optical Mini-Workshop, SeaBAM⁴)

built on the contributions from users with *in situ* measurements from the world oceans. The data consist of reflectances and chlorophyll-*a* concentrations. The *in situ* chlorophyll-*a* concentrations are plotted against ratios of reflectances at selected wavelengths and a polynomial fit is applied to the data. Two empirical algorithms, referred to as Ocean Chlorophyll (OC) 2 and 4, have emerged from these analyses⁵. Reflectance ratios are then related to ratios of water-leaving radiances in the SeaWiFS algorithms. These algorithms are designed for application at the global scale. However, many authors have emphasised the need for local algorithms to improve the measurements of chlorophyll-*a* concentration from space, especially in coastal waters and in waters where the major phytoplankton species are known to have optical properties that differ from what is taken to be the norm⁶⁻⁹. Furthermore, it is desirable to base algorithms on a sound theoretical basis, rather than on a purely empirical approach.

In this paper, a theoretical reflectance model¹⁰ is implemented with inherent optical properties¹¹ (IOP) measured locally. The model is used to compute the chlorophyll-*a* concentration in the Northwest Atlantic Ocean. This model is then extended to the near infrared to refine the atmospheric correction, as suggested by Fuentes-Yaco *et al.*¹². The new algorithm is evaluated by comparison of retrieved chlorophyll-*a* concentrations with *in situ* measurements. As in Fuentes-Yaco *et al.*¹², the analysis was carried out for three seasons (Spring, Summer and Autumn) to account for the seasonal variation in the IOPs (absorption by phytoplankton and detritus).

2. Bio-optical model of ocean colour

The algorithm proposed here is based on a theoretical ocean-colour model^{6,13,14}, and uses inherent optical properties (absorption and scattering) of the water to compute reflectances at SeaWiFS wavelengths.

2.1. Ocean-colour model in the visible

Intrinsic ocean colour was determined by spectral variations in reflectance at the sea surface. Reflectance is defined as the ratio of upwelling irradiance (radiant flux per unit area) to downwelling irradiance at the same depth:

$$R(\lambda, z) = \frac{E_u(\lambda, z)}{E_d(\lambda, z)}, \quad \dots (1)$$

where $R(\lambda, z)$ is the reflectance at wavelength λ and depth z , $E_u(\lambda, z)$ the upwelling irradiance (W m^{-2}) and $E_d(\lambda, z)$ the corresponding downwelling irradiance at the same wavelength and depth. In the model used here, the reflectance at sea surface has two components: one (R^E) due to elastic scattering (where the scattered photon has the same wavelength as the incident photon) and the other (R^R) due to Raman scattering¹⁵⁻¹⁸ (an inelastic process which implies a change in the wavelength in the scattered photon).

Using the inherent optical properties of the seawater, the elastic reflectance, R^E , at the sea surface $z=0$ can be expressed as⁶,

$$R^E(\lambda, 0) = r \frac{b_b(\lambda)}{a(\lambda) + b_b(\lambda)}, \quad \dots (2)$$

where $a(\lambda)$ and $b_b(\lambda)$ are respectively the absorption and backscattering coefficients of seawater and r is a proportionality factor¹⁹ that depends on the zenith and viewing angles, the sea state and the wavelength²⁰⁻²³. Reflectance due to Raman scattering was computed as in Sathyendranath & Platt¹⁴.

In the context of remote sensing, it is common to deal with remote-sensing reflectance, R_{RS} , which is closely related to the sea-surface reflectance R , but makes use of upwelling radiance (L_u) (flux per unit area and per unit solid angle, $\text{W m}^{-2} \text{sr}^{-1}$), rather than irradiance, and is defined as:

$$R_{RS}(\lambda, 0) = \frac{L_u(\theta, \phi, \lambda, 0)}{E_d(\lambda, 0)}. \quad \dots (3)$$

The arguments θ (zenith angle) and ϕ (azimuth angle) on the radiance indicate that the water-leaving radiance can vary with the viewing angle.

2.2. Inherent optical properties of the Northwest Atlantic Zone

The reflectance model used to compute the chlorophyll-*a* concentration was designed for Case I waters²⁴, that is to say, those waters in which phytoplankton and covarying substances may be assumed to be the principal agents responsible for variations in the optical properties of the water (backscattering and absorption).

In situ measurements were used here to determine the absorption coefficients of chlorophyll-*a*, dissolved organic matter (also referred to as yellow substance) and detritus. All the samples were collected in the Northwest Atlantic Zone (NWAZ, between 39° and 62.5° North and between 42° and 71° West, Fig. 1) during various cruises from 1996 to 2001. A total of

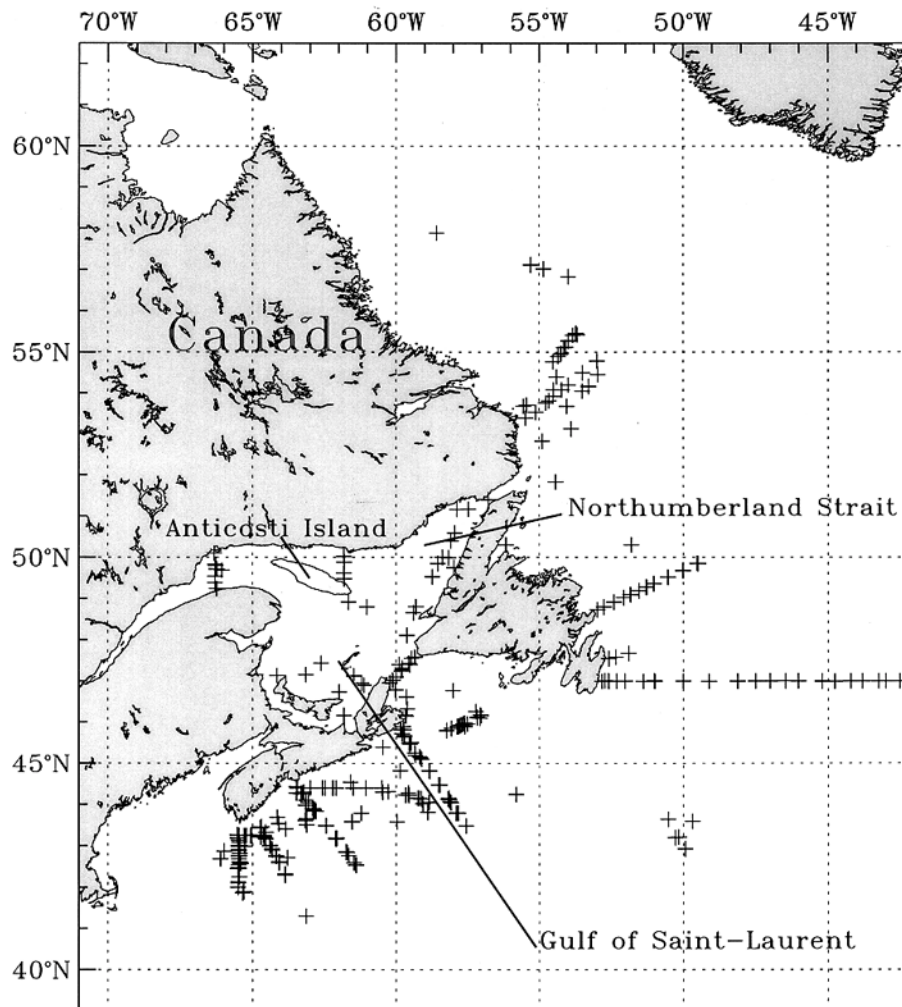


Fig. 1 — Location of the sampling stations.

847 phytoplankton samples were available, of which 455 were collected in the Spring (March, April and May), 167 in the Summer (June, July and August) and 225 in the Autumn (September, October and November). The chlorophyll-*a* concentration was estimated using a Turner Design fluorometer.

The spectral values of phytoplankton absorption coefficients were determined using the filter technique of Yentsch²⁵, as modified by Mitchell & Kiefer^{26,27} and the correction for path-length amplification was applied^{28,29} with the modification introduced by Kyewalyanga *et al.*³⁰. The phytoplankton absorption coefficient was estimated as the difference between the absorption coefficient of total particulate matter retained on the filter and the absorption coefficient of detritus measured after pigment extraction. Absorption by the detrital component was estimated according to Kishino *et al.*³¹, with some minor modifications^{32,33}. Spectral

absorption coefficients of yellow substances were also measured within two hours of sample collection during a cruise in the Autumn (26 October-07 November, 2001). Seawater was filtered using a 0.2 μm nucleopore filter and the absorption of the sample was measured using a DU[®]-64 spectrophotometer with a spectral resolution of 0.5 nm from 250 to 750 nm.

The phytoplankton absorption coefficients were parameterised as in Sathyendranath *et al.*⁶. The parameterisation assumes two chlorophyll concentrations C_1 and C_2 such that the total concentration $C=C_1+C_2$. Furthermore, it is assumed that C_1 has a finite attainable maximum value, C_1^{max} , such that $C=C_1^{\text{max}}[1-\exp(-SC)]$ where C_1^{max} and S are both unknown parameters. Since the absorption coefficients are additive, it follows that $a_c(\lambda)=a_1^*(\lambda)C_1+a_2^*(\lambda)C_2$, where $a_1^*(\lambda)$ and $a_2^*(\lambda)$ are respectively the specific absorption coefficients

(absorption coefficient normalised to the chlorophyll-*a* concentration) of the two populations. The total absorption coefficient of the whole population can then be expressed as:

$$a_c(\lambda) = U[1 - \exp(-SC)] + a_2^*(\lambda)C, \quad \dots (4)$$

where $(\lambda) = C_1^{\max}(a_1^*(\lambda) - a_2^*(\lambda))$. This equation has three free parameters that depend on λ : U , S and a_2^* . To estimate the parameters, we used the *in situ* data base of phytoplankton absorption spectra and chlorophyll-*a* concentration. Equation (4) was fitted to the data for all the SeaWiFS visible wavelengths and their corresponding Raman source wavelengths. The parameter values obtained are listed in Table 1 for the three seasons.

The absorption spectrum of yellow substance follows an exponential law³⁴,

$$a_y(\lambda) = a_y(\lambda_0) \exp(-s(\lambda - \lambda_0)), \quad \dots (5)$$

where $a_y(\lambda_0)$ is the combined absorption coefficient of yellow substance and detritus at a reference wavelength λ_0 , and s is the slope of the exponential. We have taken 440 nm as the reference wavelength here. For Case I waters, various authors have reported $a_y(440)$ values that range between 20 and 50% of $a_c(440)$ and an average of 0.014 for the slope s , with a range³⁴⁻³⁸ between 0.011 and 0.020. Equation (5) was fitted to the *in situ* database of absorption spectra of detritus and yellow substance mentioned previously. The absorption by yellow substance at 440 nm ranges between 2.4% and 30% of the phytoplankton absorption for the Autumn season with an average of 12.5%. This value is low compared to the values

found in the literature and cannot be extended to the Spring and Summer seasons. Therefore, the absorption by yellow substance was treated as a parameter to adjust the reflectance model for the NWAZ. Based on a sensitivity analysis, the proportion of absorption by yellow substance at 440 nm to that by phytoplankton for the Spring, Summer and Autumn seasons are taken to be 20%, 10% and 30% respectively, which is consistent with values found in literature.

Values of s and the ratio of $a_d(440)$ (detritus absorption) to $a_c(440)$ were estimated for all the *in situ* data. The average of s and the ratios were computed for each season. The results are presented in Table 2. These values were used in the seasonal model. The same value of s was used for absorption by yellow substances and detritus. One observes a large variability in the $a_d(440)/a_c(440)$ ratio with seasons. The Spring and the Autumn data exhibit the highest values (up to 25%). The Summer season shows a lower value (17%) perhaps as a result of photodegradation of the material. The slope, s , of the exponential is close to the average values found in the literature. The relative absorption of yellow substances and detritus were then added to compute the total absorption by the non-living matter. The relative combined absorption by yellow substances and detrital material at 440 nm to that by phytoplankton was found to be 44%, 27% and 55% respectively for the Spring, Summer and Autumn seasons.

Absorption by pure seawater was estimated according to Pope & Fry³⁹. The total absorption coefficient is then expressed as the sum of each component:

Table 1 — The parameters U (m^{-1}), $a_2^*(\lambda)$ (m^2 (mg Chl-*a*)⁻¹) and S (m^{-3} (mg Chl-*a*)⁻¹) of Eq. (4) for Spring, Summer and Autumn dataset of the Northwest Atlantic area at SeaWiFS visible wavelengths and the corresponding Raman excitation wavelengths

λ (nm)	Spring			Summer			Autumn		
	U	$a_2^*(\lambda)$	S	U	$a_2^*(\lambda)$	S	U	$a_2^*(\lambda)$	S
386	0.0302	0.0112	0.9103	0.1205	0.0036	0.3034	0.0949	0.0050	0.3565
443	0.0363	0.0108	1.0555	0.0858	0.0088	0.7858	0.1585	0.0000	0.4170
421	0.0351	0.0118	0.9109	0.0968	0.0071	0.5641	0.1606	0.0000	0.3568
490	0.0270	0.0044	1.0401	0.0496	0.0049	1.0105	0.0925	0.0000	0.4788
435	0.0368	0.0118	1.0461	0.0926	0.0085	0.7288	0.1662	0.0000	0.4033
510	0.0178	0.0036	0.9039	0.0315	0.0039	0.9074	0.0696	0.0000	0.3997
468	0.0366	0.0063	0.9764	0.0642	0.0079	0.9888	0.1256	0.0000	0.4620
555	0.0067	0.0021	0.5819	0.0078	0.0028	0.8659	0.0367	0.0000	0.3051

Table 2—Fraction of detritus absorption to chlorophyll-*a* absorption at 440 nm for three seasons in the Northwest Atlantic Zone. The slope *s* of the exponential decrease of the detritus absorption with the wavelength is also indicated with the standard error.

	Spring	Summer	Autumn
$a_d(440)/a_c(440)$ (%)	24	17	25
<i>s</i>	0.013±0.003	0.012±0.003	0.009±0.003

$$a(\lambda) = a_w(\lambda) + a_c(\lambda) + a_y(\lambda) + a_d(\lambda), \quad \dots (6)$$

where the subscript *w* stands for pure water, *c* for chlorophyll-*a*, *y* for yellow substances and *d* for detritus. Similar to the absorption coefficient, the backscattering coefficient is expressed as a sum of its components:

$$b_b(\lambda) = b_{b,w}(\lambda) + b_{b,c}(\lambda), \quad \dots (7)$$

where b_b , $b_{b,w}$ and $b_{b,c}$ represent the total backscattering coefficient, the pure seawater and phytoplankton backscattering coefficients respectively at the wavelength λ . Backscattering by water was computed according to Morel & Gordon⁴⁰. Backscattering by particles was evaluated as described in Sathyendranath *et al.*⁶.

3. Selection of reflectance ratio

The model of Sathyendranath *et al.*⁶ adapted to the NWAZ was used to compute chlorophyll-*a* concentrations using SeaWiFS normalised water-leaving radiances. These satellite-derived chlorophyll-*a* concentrations were compared with *in situ* data. The *in situ* dataset (see Fuentes-Yaco *et al.*¹², for more details) was divided into three seasons to account for the variations in the bio-optical properties. The dates and geographic coordinates of *in situ* phytoplankton concentration collected in the NWAZ between 1996 and 2001 were used to match *in situ* and satellite data. They form a set of 453 data points for the Spring, Summer and Autumn seasons (Fig. 1). The winter dataset of seven observations was too small to provide relevant statistics, and was not examined in this paper. The SeaWiFS images that correspond to the dates of sample collections were selected. For each image, the normalised water-leaving radiances at 443, 490, 510 and 555 nm were extracted from the pixels that matched the coordinates of the *in situ* measurements. The average of a 3×3 matrix centred on the selected pixel was computed. The matrices were sorted

according to the criteria defined by NASA⁴ and Fuentes-Yaco *et al.*¹² and all the matrixes presenting anomalies were removed (e.g., cloud, negative chlorophyll-*a* values). Pixels that passed the following criteria were used for the match-up:

1. Viewing angle selection: pixels that have a viewing angle lower than 56°;
2. Minimum number of valid pixels: the matrix has five or more pixels with positive chlorophyll-*a* concentration values;
3. Cloud albedo selection: pixels with a cloud albedo lower than $0.6+2\sigma$ (where σ is the standard deviation of the remaining pixels after the step 1 and 2);
4. Large coefficient of variation elimination: the pixels with chlorophyll-*a* concentration greater (or less) than the matrix average chlorophyll-*a* concentration plus (or minus) two times the coefficient of variation were eliminated from the analysis.

The relevance of the selection criteria is discussed in detail in Fuentes-Yaco *et al.*¹². From an initial set of 194 data points for the Spring season, only 110 satisfied these additional selection criteria (42 out of 86 for the Summer and 33 out of 173 for the Fall). The satellite-derived chlorophyll-*a* concentration was estimated using the theoretical model and SeaWiFS water-leaving radiances. Several water-leaving radiances ratios were tested: $[L_w(443)]_n/[L_w(555)]_n$, $[L_w(490)]_n/[L_w(555)]_n$ and $[L_w(510)]_n/[L_w(555)]_n$, where $[L_w(\lambda)]_n$ refers to the normalised SeaWiFS water-leaving radiance at the wavelength λ . The satellite-derived chlorophyll-*a* concentrations are plotted against the *in situ* data in Fig. 2 for the three water-leaving radiance ratios for the Spring season. A Weighted Deming Regression (WDR) analysis^{41,42} was performed on the data (see Appendix for details) to compute the slope, *a*, and the intercept, *b*, of a linear fit on the data,

$$C_s = aC_m + b, \quad \dots (8)$$

where C_s and C_m are respectively the satellite-derived and *in situ* chlorophyll-*a* concentrations. The parameters *a* and *b* that correspond respectively to the intercept with the ordinate axis and the slope of the fit are summarised in the Table 3.

The WDR analysis was applied on raw data (not log-transformed), which is more relevant for the analysis of the performance of the model. A curvature of the fit close to the origin in the plot can be observed in Fig. 2 due to a logarithmic scale chosen

Table 3—Results of the comparison of satellite-derived chlorophyll-*a* versus the *in situ* chlorophyll-*a* concentration. The satellite-derived concentration is computed using the theoretical reflectance model and the SeaWiFS water-leaving radiances ratios: 443:555, 490:555, 510:555. The coefficients of the fit $C_s = aC_m + b$ where C_s and C_m are respectively the satellite-derived and *in situ* chlorophyll-*a* concentrations are shown. The standard deviation, σ , and the weighted correlation coefficient, r_w^2 , are also indicated.

Reflectance ratio	443:555	490:555	510:555
a	2.242	1.602	1.160
b	-0.823	-0.319	-0.204
s (mg m^{-3})	0.305	0.279	0.254
r_w^2	0.438	0.636	0.653

for more clarity in the presentation. At 443 nm, the satellite-derived data clearly overestimated the chlorophyll-*a* concentration, especially at low chlorophyll-*a* concentrations. Failure of the atmospheric correction algorithm is a potential source for the bias. This possibility is further explained in section 4.1.

The $[L_w(490)]_n/[L_w(555)]_n$ ratio gives better results than the $[L_w(443)]_n/[L_w(555)]_n$ ratio with a higher correlation coefficient, 0.636 compared to 0.438. Although the bias is reduced, an overestimation of the chlorophyll-*a* concentration is still observed ($a=1.602$). The $[L_w(510)]_n/[L_w(555)]_n$ ratio yields the best results. The linear fit is close to the 1:1 line, $a=1.160$, with a low intercept ($b=-0.204$) and high correlation coefficient, $r^2=0.653$. The phytoplankton concentration computed using the $[L_w(670)]_n/[L_w(555)]_n$ ratio globally underestimates the measured concentration ($a=0.806$) except at low chlorophyll-*a* concentration (results not shown here).

The $[L_w(510)]_n/[L_w(555)]_n$ ratio yields the best comparison with the *in situ* data. The $[L_w(490)]_n/[L_w(555)]_n$ ratio gives promising results as well but with a systematic bias in the estimated chlorophyll-*a* concentration. Atmospheric correction is a critical step when estimating chlorophyll-*a* concentrations: a potential overestimation of the aerosol signal can lead to an underestimation of the water-leaving radiances at short wavelengths, which can then result in an overestimation of chlorophyll-*a* concentration. In the next section, we address the atmospheric correction problem and particularly the estimation of the phytoplankton contribution to the total signal in the near infrared, which in turn is used to compute the atmospheric radiances in the visible.

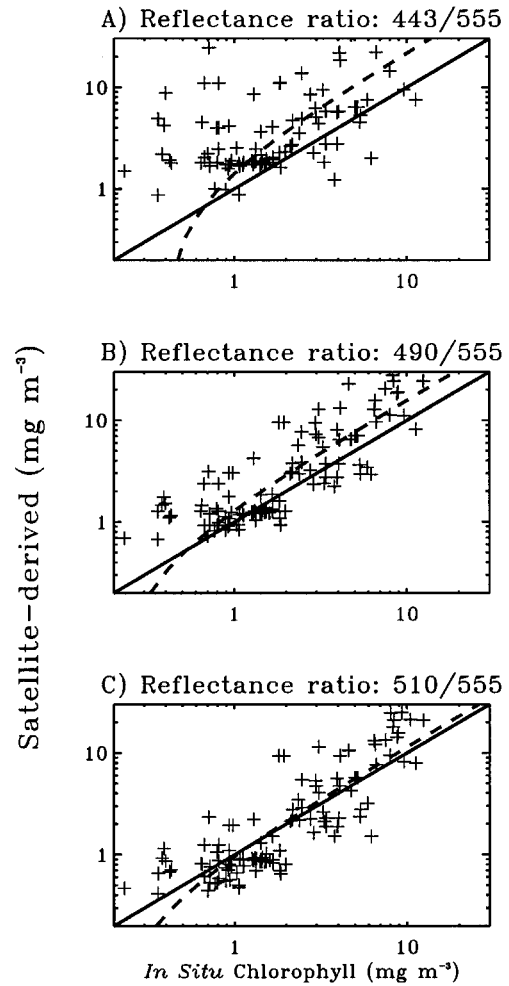


Fig. 2— Comparison between satellite-derived chlorophyll-*a* and the *in situ* chlorophyll-*a* for the Spring season. The satellite-derived chlorophyll-*a* was computed using the SeaWiFS water-leaving radiance ratios 443, 490 and 510 nm to 555 nm and the theoretical reflectance model. The solid line corresponds to the 1:1 line and the dashed line corresponds to the fit $C_s = aC_m + b$ where C_s and C_m are the satellite-derived and *in situ* chlorophyll-*a* concentration respectively, and the coefficients a and b are summarised in the Table 3.

4. Application of NIR model to SeaWiFS data.

4.11. Extension of the model to the near infrared

Besides the computation of the marine reflectances in the visible spectrum, the theoretical reflectance model was used to assess the marine contribution to the total signal at the top-of-atmosphere (TOA) in the near-infrared (NIR) for atmospheric correction purposes. The absorption by yellow substances, detritus and chlorophyll-*a* is null in the NIR such that only the absorption and backscattering by pure seawater and the backscattering by phytoplankton affect the signal reaching the satellite. The scattering

by phytoplankton in the NIR was computed using the bio-optical model described in the previous section extrapolated into the NIR. The NASA reflectance model³ in the NIR was replaced by this model when processing the raw SeaWiFS data (Level 1) to get the geophysical data (Level 2).

The contribution of the Raman scattering by phytoplankton to the total signal in the near infrared was computed according to Sathyendranath & Platt¹⁴. However, the inclusion of Raman scattering did not improve the results (not shown here) in agreement with the works of other authors^{6, 43, 44}.

To apply the atmospheric correction algorithm, it is necessary to compute the remote sensing reflectance as described in Eq. (3). As shown by Morel & Gentili²², the upwelling irradiance is related to the water-leaving radiance according to,

$$E_u(0) = Q \times L_u(0, \theta', \Phi), \quad \dots (9)$$

so that,

$$R_{RS}(0, \theta', \Phi) = R(0, \theta', \Phi) / Q, \quad \dots (10)$$

where θ and Φ are respectively the zenith and azimuthal angles of propagation of the radiance. The coefficient Q is known to vary from 3 to more than 5 according to the sun zenith angle, the direction of propagation of the water-leaving radiances, the seawater composition and the sea surface state. The dependence of Q on the solar zenith angle was modelled according to Åas & Højerslev⁴⁵ and the dependence on chlorophyll-*a* concentration was taken from Morel & Gentili²³. This parameterisation of Q gives a minimal value of 3.3 at low chlorophyll-*a* concentration and for a sun at zenith, and a maximal value of more than 6.5 at high solar zenith angle and high chlorophyll-*a* concentration (Fig. 3). The model for Q extrapolated to the NIR was coupled with the theoretical reflectance model to compute the remote-sensing reflectance in the NIR. As described in Siegel *et al.*³, the marine signal in the NIR is computed using an iterative procedure with an initial chlorophyll-*a* concentration of 0.2 mg m⁻². Thus, the reflectance model used to estimate the chlorophyll-*a* concentration is also involved in the atmospheric correction procedure. In these computations, the NASA/SeaDAS OC4 model was replaced by the semi-analytical reflectance model. The maximum chlorophyll-*a* concentration was set to 40 mg m⁻³ instead of the threshold value of 64 mg m⁻³ in SeaDAS.

4.2. Results for the spring season

The satellite-derived chlorophyll-*a* concentrations were recomputed using the 510:555 water-leaving radiances ratio and the modified atmospheric correction procedure as described in the previous paragraph. The results for the Spring season are plotted in Fig. 4. A linear fit according to Eq. (8) was performed. The parameters of the fit are summarised in Table 4. The intercept and the slope of the fit for the Spring season are substantially improved compared with the case without the modified atmospheric correction (slope of 0.999 and intercept of 0.0296). We also examined the values of negative

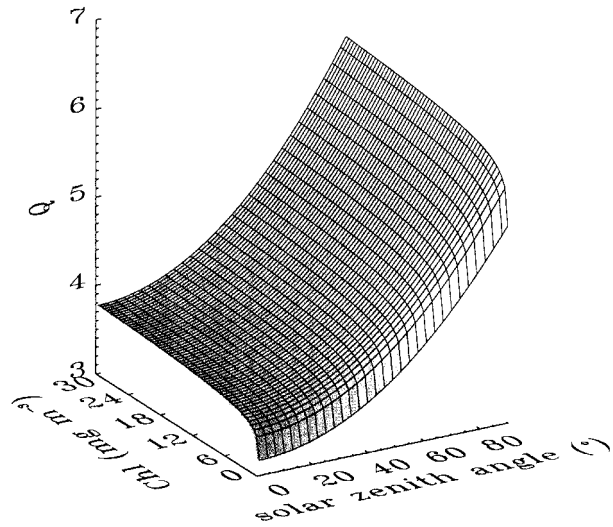


Fig. 3 — Variation of the Q factor with the solar zenith angle⁴⁵ and the chlorophyll-*a* concentration²³.

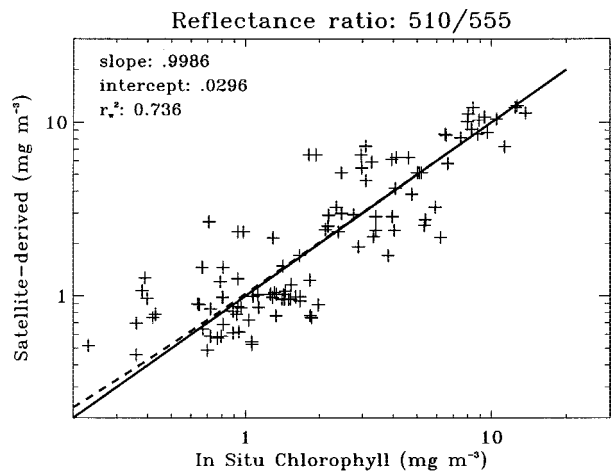


Fig. 4 — Comparison of the satellite-derived chlorophyll-*a* concentration computed using the theoretical model and the modified atmospheric correction versus the *in situ* chlorophyll-*a* concentration for the Spring season. The dashed line corresponds to a linear fit and the solid line corresponds to the 1:1 line.

Table 4 — Coefficients of the fit $C_s = aC_m + b$ where C_s and C_m are respectively the satellite-derived and *in situ* chlorophyll-*a* concentration computed using the theoretical reflectance model and the NASA OC4 algorithm (in brackets). The standard deviation and the weighted correlation coefficient are also indicated.

	Spring (OC4)	Summer (OC4)	Fall (OC4)
Number of data	110	42	33
a	0.999 (0.50)	0.825 (0.673)	0.661 (0.632)
b	0.0296 (0.2814)	0.039 (0.140)	0.330 (0.4942)
s (mg m^{-3})	3.303 (2.188)	0.368 (0.347)	0.975 (0.715)
r_w^2	0.736 (0.706)	0.696 (0.723)	0.855 (0.823)

water-leaving radiances at 443, 490, 510, 555 and 670 nm that result from the failure of the atmospheric corrections procedure. The results are summarised in Table 5 for both the NASA procedure and for the modified version for a SeaWiFS image of April 19th 1998 for the Northwest Atlantic Zone. The number of negative pixels (%) decreases at short wavelengths.

These results support the idea of a non-negligible contribution of the marine signal to the TOA signal in the near infrared, even at low chlorophyll-*a* concentrations, that influences the atmospheric correction scheme. The 443 nm band corresponds to the chlorophyll-*a* absorption peak such that the water-leaving radiances at this wavelength are very low. Then, a slight decrease of the atmospheric signal leads to an increase in the water-leaving radiances and a decrease in the number of negative values. At the same time, the average chlorophyll-*a* concentration for the whole image increased by almost a factor two ($2.6 \text{ mg Chl m}^{-3}$ using OC4 versus $4.6 \text{ mg Chl m}^{-3}$ using the theoretical model and the modified atmospheric correction procedure). This increase results from the use of the theoretical reflectance model to retrieve the chlorophyll-*a* concentration.

Both the NASA and the theoretical algorithms were applied to SeaWiFS raw data (L1A level) to compute the chlorophyll-*a* concentration (Fig. 5). The image of April 19th 1998 was used as in the work of Fuentes-Yaco *et al.*¹² to facilitate the comparison. In Fig. 5B (chlorophyll-*a* concentrations computed using the regional reflectance model), spring bloom can be seen at the bottom centre of the picture (also labelled as Bloom in Fig 5B), with values of chlorophyll-*a* concentration up to 25 mg m^{-3} , whereas Fig. 5A (chlorophyll-*a* concentration computed using OC4) shows lower chlorophyll-*a* concentrations close to 5 mg m^{-3} . At this time of the year (April) in this area, high chlorophyll-*a* concentrations are found when the

Table 5 — Number of pixels with negative normalised water-leaving radiance values computed using the NASA procedure and the theoretical model with the modified atmospheric correction scheme, the fourth column corresponds to the decrease of negative values (%), the last row corresponds to the mean chlorophyll-*a* concentration for the whole image on 19 April 1998. C_{SARM} stands for chlorophyll-*a* concentration computed using the Semi-Analytical Reflectance Model.

l (nm)	$[L_w]_n, \text{NASA}$ [$\text{mW m}^{-1} \mu\text{m}^{-1}$ sr^{-1}]	$[L_w]$ n,SARM [mW m^{-1} $\mu\text{m}^{-1} \text{sr}^{-1}$]	Decrease in number of negative pixels (%)
412	386747	312972	53.0
443	61610	28954	41.6
490	5997	4303	-1.1
510	4263	2915	-1.0
555	2463	1559	0.0
670	115787	115108	0.6
C_{NASA} (mg m^{-3})	C_{SARM} (mg m^{-3})		
2.6	4.6		

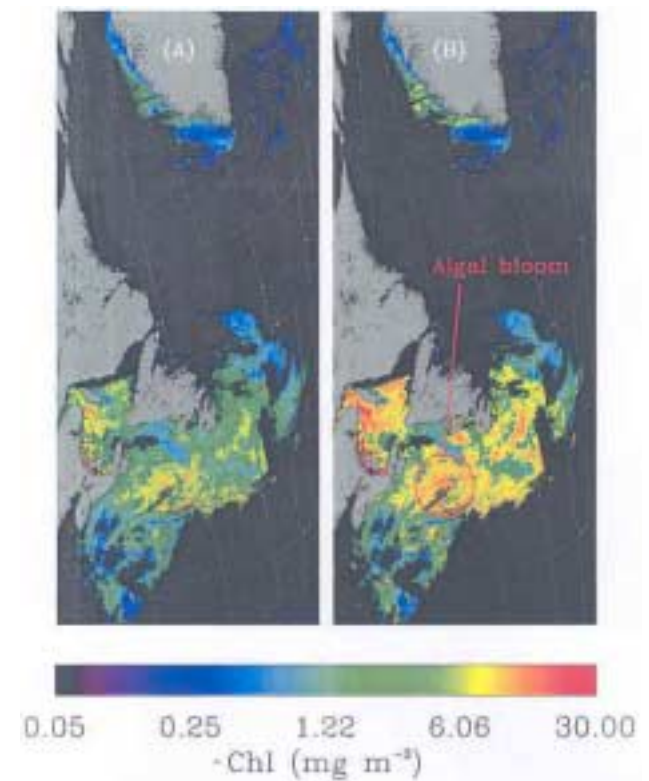


Fig. 5 — Chlorophyll concentration on April 19th 1998 in the Northwest Atlantic region computed with the OC4 algorithm (A) and the theoretical model (B).

day length is long and nutrients are available for the growth of phytoplankton. Although no measurements inside the bloom area are available, concentrations close to 20 mg m^{-3} are more likely than the low concentrations given by the NASA model. We notice the failure of the theoretical model close to the shore (white pixels), south of Anticosti Island (mouth of the Saint-Laurent River) and Northumberland Strait, probably caused by the Case II type of waters in these regions with the presence of mineral particles and other substances that were not taken into account in the theoretical model.

4.3. Summer and Autumn seasons

The same method that was used for the Spring season was applied to the Summer and Autumn seasons (Fig. 6). The slope and intercept of comparisons between computations and observations are summarised in Table 4 for both OC4 and the theoretical model. The local algorithm exhibits a higher slope and a lower intercept than the NASA algorithm (0.825 versus 0.673 and 0.039 versus 0.140 respectively) for the Summer season. The results are slightly improved for the Autumn season but with similar slopes (0.661 and 0.632 respectively for the

theoretical model and OC4) but the intercept is closer to zero for the theoretical model.

5. Discussion

Fuentes-Yaco *et al.*¹² demonstrated some of the limitations of the NASA/SeaDAS OC2 and OC4 algorithms when applied to the Northwest Atlantic Zone. The solutions they proposed were the division of the year into periods to account for the change in the inherent optical properties, the use of a reflectance model based on the radiative transfer theory and the improvement of the atmospheric correction procedure. These issues are addressed in this paper and computations are compared with *in situ* data. Three distinct seasons are considered: Spring, Summer and Autumn, with different parameterisations of the optical contributions of phytoplankton and other organic material. The model, tested on the Spring data, showed that the use of the 510:555 reflectance ratio yielded the best results compared with other band ratios. Even though the theoretical model gave better results than the NASA OC2 and OC4 algorithms for the Spring season, it also underlined some limitations of the atmospheric correction procedure.

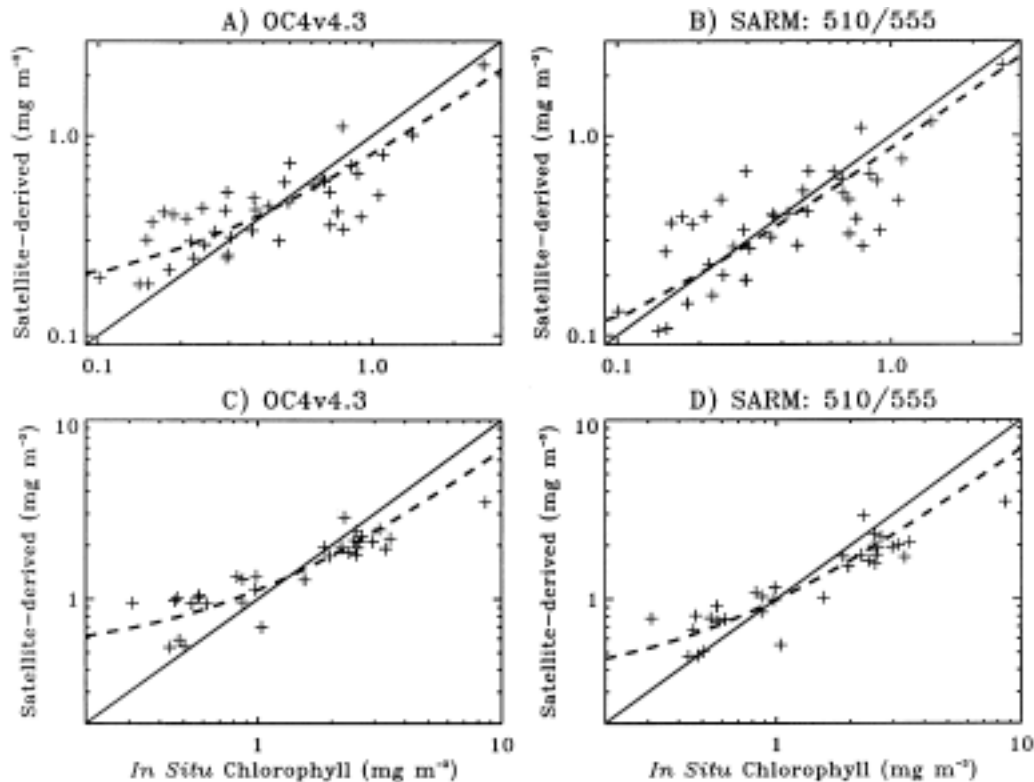


Fig. 6 — Satellite-derived Chl computed with the OC4 algorithm (A and C) and with the theoretical reflectance model (Fig. B and D) for the Summer (top) and Fall (bottom) seasons versus the *in situ* Chl data. The legend is the same as for Fig. 2.

The results were further improved with a modified algorithm to compute the contribution of water to the signal at the top of atmosphere in the near infrared. This modification to the atmospheric correction procedure resulted in a substantial decrease in the number of negative normalised water-leaving radiances. Moreover, the chlorophyll-*a* concentration computed using this approach for all seasons compared well with *in situ* measurements.

This work emphasises the need for local models of ocean colour that take into account the regional optical properties. The division of the optical properties of phytoplankton and other organic material according to the season appears to improve the results further. The variability in the ratio of the detrital absorption coefficient to the chlorophyll-*a* absorption coefficient remains a problem even in the open ocean where high concentrations of detrital material were found. These issues merit further attention.

Improved chlorophyll-*a* retrieval will lead to better estimations of other products such as primary production at large temporal and spatial scales. The model used here for the Northwest Atlantic region can be easily adapted to other oceans provided that the inherent optical properties for the region are well known.

Appendix

A. Weighted Deming Regression analysis

The statistical method used here to compare the chlorophyll-*a* concentration data is borrowed from medical biochemistry. It is designed for use when it is necessary to compare different instruments, which measure the same quantities with different methods. In this method, it is recognised that different uncertainties exist for the different instruments and methods. The Weighted Deming Regression analysis (WDR) is briefly described here⁴². The computations were performed using the CBstat software developed by K. Linnet [available at <http://www.cbstat.com>]

The WDR analysis is based on the minimisation of the distance between a data pair (X, Y) and the regression line according to an angle determined by the squared error ratio, unlike the usual linear least-square regression which results in a bias of the regression line toward the x-axis. Moreover, the WDR analysis optimises the regression in the case of a non-constant error of the instrument. Such errors are frequent in satellite measurements, for instance, due

to the atmospheric correction procedure or changes in phytoplankton species. The WDR method applies a weighting that prevents a strong influence by the high values, which often result in a regression line away from (0,0). An estimation of the standard error of the slope and intercept is computed using the jackknife procedure^{41,46}. The weight, the slope and the intercept are computed as follows:

$$w_i = 1 / [0.5(X_i + Y_i)^2], \quad \dots (11)$$

where X_i and Y_i correspond to the two measurements of a quantity by two different methods (the chlorophyll-*a* concentration in our case). The weight, w_i , is introduced as the sum of squared deviations and cross-products. As the X_i and Y_i are unknown true values, a weighted estimate is obtained according to:

$$w_i = 1 / [0.5(X_{esti} + Y_{esti})(1 + \lambda)]^2, \quad \dots (12)$$

where $\lambda = \sigma_x^2 / \sigma_y^2$, σ_x^2 and σ_y^2 are respectively the analytical standard deviation of the X_i and Y_i dataset. The weighted averages are then computed as

$$X_{wm} = \sum w_i X_i / \sum w_i \quad \dots (13)$$

and

$$Y_{wm} = \sum w_i Y_i / \sum w_i \quad \dots (14)$$

and the weighted square deviation and cross-products are summed:

$$u_w = \sum w_i (x_i - x_{mw})^2, \quad \dots (15)$$

$$q_w = \sum w_i (y_i - y_{mw})^2 \quad \dots (16)$$

and

$$p_w = \sum (x_i - x_{mw})(y_i - y_{mw}) \quad \dots (17)$$

The slope estimate is:

$$a = \left[\lambda q_w - u_w + \sqrt{(u_w - q_w)^2 + 4\lambda p_w^2} \right] / 2\lambda p_w \quad \dots (18)$$

and the intercept is equal to:

$$b = y_{mw} \quad \dots (19)$$

The weighted product-moment of correlation (r_w^2) is computed as:

$$r_w^2 = p_w / (u_w q_w)^{0.5}. \quad \dots (20)$$

Acknowledgement

This work was carried out as part of the Canadian SOLAS project. This work was also supported by the Canadian Space Agency and the Department of

Fisheries and Ocean, Canada. The ocean-colour data used in this study were provided by the SeaWiFS project at Goddard Space Flight Centre. The data were obtained from the Goddard Distributed Active Archive Centre. Use of this data is in accordance with the SeaWiFS Research Data Use Terms and Conditions Agreement.

References

- Hooker S B & McClain C R, The calibration and validation of SeaWiFS data, *Prog. Oceanogr.*, 45 (2000) 427–465.
- Wang M & Gordon H R, A simple, moderately accurate, atmospheric correction algorithm for SeaWiFS, *Int. J. Remote Sens.*, 16 (1994) 231–239.
- Siegel D A, Wang W, Maritorena S & Robinson W, Atmospheric correction of satellite ocean color imagery: the black pixel assumption, *Appl. Opt.*, 39 (2000) 3582–3591.
- McClain C R, Barnes R A, Eplee R E, Franz B A, Hsu N C, Patt F S, Pietras C M, Robinson W D, Schieber B D, Schmidt G M, Wang M, Bailey S W & Werdell P J, Normalised water-leaving radiances and chlorophyll-*a* concentration match-up analyses, in *SeaWiFS Postlaunch Technical Report Series, SeaWiFS Postlaunch Calibration and Validation Analyses, Part 2.*, vol. 10, edited by S. B. Hooker & E. R. Firestone (NASA, Goddard Space Flight Center, Greenbelt, Maryland) (2000) pp. 45–52.
- O'Reilly J E, Maritorena S, Mitchell B G, Siegel D A, Carder K L, Garver S A, Kahru M & McClain C, Ocean color chlorophyll algorithm for SeaWiFS, *J. Geophys. Res.*, 103 (1998) 24, 937–24, 953.
- Chuqun, C., Ping S, Larson M & Jonsson L, Applications of SeaWiFS data for determination of chlorophyll-*a* concentration in the Pearl River estuary, in Guangdong, China, The Fifth Pacific Ocean Remote Sensing Conference (PORSEC) Proceedings vol 1., (National Institute of Oceanography, Dona Paul, Goa, India) 2000, pp. 94–99.
- Burenkov, V I, Verdernikov V I, Ershova S V, Kopelevitch O V & Sheberstov S V, Use of satellite ocean color data for assessment of bio-optical characteristics in the Barents Sea, *Okeanologiya*, 41 (2001) 485–492.
- Reynolds R A, Stramski D, & Mitchell B G, A chlorophyll-dependent semi-analytical reflectance model derived from field measurements of absorption and backscattering coefficients within the Southern Ocean, *J. Geophys. Res.*, 106 (2001) 7125–7138.
- Gohin F, Druon J N & Lampert L, A five channel chlorophyll concentration algorithm applied to SeaWiFS data processed by SeaDAS in coastal waters, *Int. J. Remote Sens.*, 23 (2002) 1639–1661.
- Sathyendranath S, Cota G, Stuart V, Maass H & Platt T, Remote sensing of phytoplankton pigments: a comparison of empirical and theoretical approaches, *Int. J. Remote Sensing*, 22 (2001) 249–273.
- Preisendorfer R W, *Hydrologic optics*, Vol. 5: *Properties* (Environment Research Laboratory, National Oceanic and Atmospheric Administration, U.S. Department of Commerce, Washington D.C.) 1976, pp. 10.
- Fuentes-Yaco, C, Devred E, Sathyendranath S, Platt T, Payzant L, Caverhill C, Porter C, Maass H, White J G, Comparison of *in situ* and remotely-sensed (SeaWiFS) chlorophyll-*a* in the Northwest Atlantic, *Indian J. Mar. Sci.*, 34 (2005) 341–355.
- Sathyendranath S & Platt T, Analytic model of ocean-colour, *Appl. Opt.*, 36 (1997) 2620–2629.
- Sathyendranath S & Platt T, Ocean-colour model incorporating transpectral processes, *Appl. Opt.*, 37 (1998) 2216–2226.
- Sugihara S, Kishino M & Okami N, Contribution of Raman scattering to upward irradiance in the sea, *J. Oceanogr. Soc. Jpn*, 40 (1984) 397–404.
- Marshall B R & Smith R C, Raman scattering and in water ocean optical properties, *Appl. Opt.*, 29 (1990) 71–84.
- Stavn R H, Effects of Raman scattering across the visible spectrum in clear ocean water: a Monte Carlo study, *Appl. Opt.*, 32 (1993) 6853–686.
- Bartlett J S, Voss K J, Sathyendranath S & Vodacek A, Raman scattering by pure water and seawater, *Appl. Opt.*, 37 (1998) 3324–3332.
- Gordon H R & McCluney W R, Estimation of the depth of sunlight penetration in the sea for remote sensing, *Appl. Opt.*, 14 (1975) 413–416.
- Kirk J T O, Dependence of relationship between inherent and apparent optical properties of waters on solar altitude, *Limnol. Oceanogr.*, 29 (1984) 350–356.
- Gordon H R, Dependence of the diffuse reflectance of natural waters on the sun angle, *Limnol. Oceanogr.*, 34 (1989) 1484–1489.
- Morel A & Gentili B, Diffuse reflectance of oceanic waters. II. Bidirectional aspects, *Appl. Opt.*, 32 (1993) 6864–6879.
- Morel A & Gentili B, Diffuse reflectance of oceanic waters. III. Implication of bidirectionality for the remote-sensing problem, *Appl. Opt.*, 35 (1996) 4850–4862.
- Morel A & Prieur L, Analysis of variation in ocean color, *Limnol. Oceanogr.*, 22 (1977) 709–722.
- Yentsch C S, Measurement of visible light absorption by particulate matter in the ocean, *Limnol. Oceanogr.*, 7 (1962) 207–217.
- Mitchell B G & Kiefer B A, Determination of absorption and fluorescence excitation spectra for phytoplankton, in *Marine phytoplankton and productivity*, edited by O. Holm-Hansen, L. Bolis, & R. Giles (Springer-Verlag, Berlin Heidelberg) 1984, pp. 157–169.
- Mitchell B G & Kiefer B A, Variability in pigment specific particulate fluorescence and absorption spectra in the northeast Pacific Ocean, *Deep-Sea Res.*, 28 (1988) 1375–1393.
- Hoepffner N & Sathyendranath S, Bio-optical characteristics of coastal waters: absorption spectra of phytoplankton and pigment distribution in the western North Atlantic, *Limnol. Oceanogr.*, 37 (1992) 1660–1679.
- Hoepffner N & Sathyendranath S, Determination of the major groups of phytoplankton pigments from the absorption spectra of total particulate matter, *J. Geophys. Res.*, 98 (1993) 22, 789–22, 803.
- Kywalyanga, M N, Platt T & Sathyendranath S, Estimation of the photosynthetic action spectrum: implication for primary production models, *Mar. Ecol. Prog. Ser.*, 146 (1997) 207–223.
- Kishino M, Takahashi M, Okami N & Ichimura S, Estimation of the spectral absorption coefficients of phytoplankton in the sea, *Bull. Mar. Sci.*, 37 (1985) 634–642.

- 32 Stuart V, Sathyendranath S, Platt T, Maass H & Irwin B D, Pigments and species composition of natural phytoplankton populations: effect on the absorption spectra, *J. Plankton Res.*, 20 (1998) 187–217.
- 33 Sathyendranath S, Stuart V, Irwin B D, Maass H, Savidge G, Gilpin L & Platt T, Seasonal variation in bio-optical properties of phytoplankton in the N.W. Indian Ocean, *Deep-Sea Res.-II*, 46 (1999) 633–654.
- 34 Bricaud A, Morel A & Prieur L, Absorption by dissolved organic matter of the sea (yellow substance) in the UV and visible domains, *Limnol. Oceanogr.*, 26 (1981) 43–53.
- 35 Kopelevitch O V & Burenkov V I, Relation between the spectral values of the light absorption coefficients of sea water, phytoplanktonic pigments, and yellow substance, *Oceanology*, 17 (1977) 278–282.
- 36 Roesler C S, Perry M J & Carder K L, Modelling in-situ absorption from total absorption spectra in productive inland marine waters, *Limnol. Oceanogr.*, 34 (1989) 1510–1523.
- 37 Siegel D A & Michaels A F, Quantification of non-algal light attenuation in the Sargasso Sea: Implications for biogeochemistry and remote sensing, *Deep-Sea Res.-II*, 43 (1996) 321–345.
- 38 Bouman H, Platt T, Kraay G W, Sathyendranath S & Irwin B D, Bio-optical properties of the subtropical North Atlantic. I. Vertical variability, *Mar. Ecol. Prog. Ser.*, 200 (2000) 3–18.
- 39 Pope R M & Fry E S, Absorption spectrum (380–700 nm) of pure water. II. Integrating measurements, *Appl. Opt.*, 36 (1997) 8710–8723.
- 40 Morel A & Gordon H, Relation between total quanta and total energy for aquatic photosynthesis, *Limnol. Oceanogr.*, 19 (1974) 591–600.
- 41 Linnet K, Estimation of the linear relationship between the measurements of two methods with proportional errors, *Stat. Med.*, 9 (1990) 463–473.
- 42 Linnet K, Evaluation of regression procedures for method comparison studies, *Clin. Chem.*, 39 (1993) 424–432.
- 43 Waters A, Effects of Raman scattering on water-leaving radiance, *J. Geophys. Res.*, 96 (1991) 13, 151–13, 161.
- 44 Pozdnyakov D, Lyaskovsky A, Grassl H & Pettersson L, Numerical modelling of transpectral processes in natural waters: implications for remote sensing, *Int. J. Remote Sens.*, 23 (2002) 1581–1607.
- 45 Åas E & Højerslev N K, Analysis of underwater radiance observations: Apparent optical properties and analytic functions describing the angular radiance distribution, *J. Geophys. Res.*, 104 (1999) 8015–8024.
- 46 Wu C FJ, Jackknife, bootstrap and other resampling methods in regression analysis (with discussion) *Ann. Stat.*, 14 (1986) 1261–1295.